Hindawi
Advances in Materials Science and Engineering
Volume 2018, Article ID 2395083, 9 pages
https://doi.org/10.1155/2018/2395083

Research Article

Experimental Study on the Mechanical Properties of Amorphous Alloy Fiber-Reinforced Concrete

Chaohua Jiang, Yizhi Wang, Wenwen Guo, Chen Jin, and Min Wei

Jiangsu Key Laboratory of Coast Ocean Resources Development and Environment Security, Hohai University, No. 1 Xikang Road, Nanjing 210098, China

Correspondence should be addressed to Min Wei; 18351932989@163.com

Received 1 August 2018; Accepted 14 October 2018; Published 18 November 2018

Academic Editor: Antonio Caggiano

With great mechanical properties and corrosion resistance, amorphous alloy fiber (AAF) is a highly anticipated material in the fiber-reinforced concrete (FRC) field. In this study, the mechanical properties of AAFRC such as compressive strength, tensile strength, and flexural strength were examined. The comparison and analysis between AAFRC and steel fiber-reinforced concrete (SFRC) were also carried out. The results show that adding fibers significantly improves the concrete strength and toughness index. Compared with plain concrete, the compressive strength, splitting tensile strength, and flexural strength of AAFRC increase by 8.21–16.72%, 10.4–32.8%, and 18.12–45.21%, respectively. Meanwhile, the addition of AAF with a greater tensile strength and larger unit volume quantity improves the splitting tensile strength and flexural strength of concrete more noticeably than that of SF. Adding AAF improves the ductility of concrete more significantly in comparison to the SF. AAFRC shows great interfacial bonding performance as well. A prediction equation for the strength of AAFRC was proposed, which verified good accuracy calibrated based on the test results.

1. Introduction

At present, various types of fibers, including steel fiber (SF) and polypropylene (PP) fiber, can be used in concrete to improve its engineering properties, such as tensile strength, toughness, and durability [1]. Adding SF to the concrete can effectively improve the tensile property of the matrix and restrain crack initiation and propagation. However, SF is difficult to disperse. Furthermore, under the action of load or environmental factors, cracked SFRC is susceptible to corrode due to the cracks accelerating the intrusion of chloride ions especially in marine environments such as harbor engineering [2]. Corrosion of SF surfaces greatly reduces the bonding of the fiber and matrix, thus affecting the carrying capacity and deformation properties of the SFRC components [3]. The addition of some polymer fibers like PP fibers can significantly improve corrosion resistance, impermeability, and durability of concrete. However, the polymer fiber has a disadvantage of low strength and modulus and has poor interfacial bonding with the cement matrix. Therefore, it is indispensable to explore new and high-performance fibers to increase the tensile strength and permeability of concrete, thus improving its durability greatly, especially in the military and marine fields.

The crystalline metal can be obtained when the liquid metal is cooled slowly, and the properties can be adjusted by controlling the cooling speed [4]. But when the liquid metal is cooled at a rapid rate of more than 10^5 K/s, the metal does not have time to crystallize [5, 6]. After this process, the atoms of the amorphous metal are topologically disordered in three-dimensional spaces. Amorphous alloy fiber (AAF), or metallic glass ribbon (MGR), is a kind of banding amorphous material, which shows excellent mechanical properties, corrosion resistance, and special electromagnetic property owing to no grain boundaries or stacking faults [7]. The study on the AAF-reinforced epoxy and glass-ceramic matrix composites, respectively, was conducted as early as 1985 [8, 9]. The results showed that AAF could effectively improve the matrix strength and fracture toughness even at a rather low mixing content. The studies carried out by

Wu et al. [10] and Choi et al. [11], respectively, indicated that AAF possessed stable, amorphous, and excellent corrosion resistance in high-temperature and acid, alkali, and salt environments. After immersing for 30 days in 3.0% NaCl solution, the observed results for appearance of AAFs and SFs showed that a large amount of rust developed on the surface of the SFs, while the AAFs had not any corrosion. The good resistance to chloride erosion enables AAFs to exhibit no strength decrease for prolonged exposure to the elements.

Choi et al. [11] found that AAF has higher fiber content compared to steel, PP, and polyvinyl alcohol fiber, which benefits to the bridging in mixture. The mortar possesses better plastic-shrinkage resistance by adding AAF; the toughness and impact resistance of AAFRC could be improved significantly either. Moreover, studies on the flexural strength and bond performance of Fe-based AAFRC were conducted. Won et al. [5, 12] found that compared with hooked-end SFRC, the flexural strength and flexural deflection of AAFRC improved by about 30% and 40%, respectively, with 1% volume fraction. Meanwhile, the addition of the AAF showed more significant improvement on structure performance than that of the hooked-end steel fiber due to its larger amount and thus the larger bonding area. Lately, Kim et al. [13] conducted the studies about the effect of AAF with different embedment lengths (5.0, 8.0, and 12.5 mm) on the pull-out behavior of AAFRC. The investigation results presented that AAF with 5~8 mm embedment length displayed the strongest enhancement effect for mortar with compressive strength exceeding 40 MPa. Furthermore, the invention patent about the preparation method of a kind of modified AAFRC composite material published in 2007 showed that the modified AAFRC had advantages in specific strength, specific modulus, flexibility, and corrosion resistance compared with the plain concrete [14].

At present, amorphous alloy strips had been widely used [15, 16]; the preparation method to produce the AAF with a completely amorphous state, a controllable size, and a low cost has been proposed, which was suitable for a large number of applications in concrete engineering [17]. The unit price of AAF is 20% higher than that of the steel fiber, which will increase the initial cost of the concrete structure [18]. However, high-performance AAFRC can reduce the maintenance and repair costs of the structure in service. Yang et al. [18] found that adding pavement with 5 kg/m^3 and 10 kg/m^3 AAF could acquire 1.2 and 1.3 times longer service life compared with the ordinary concrete pavement. With the improvement of AAF preparation methods, the cost of the AAFRC structure will be further reduced; it can be expected to have a broad application prospect in the field of reinforced concrete, especially in special fields such as fortified structures, blast-resistant structures, offshore platforms, and the exploitation of undersea oil engineering. These pioneering and trial studies also indicate that the AAF shows great flexural strength and corrosion resistance, especially suitable for application in the marine engineering field. However, the fundamental performance such as the mechanical properties of AAFRC is still limited. The mechanical behavior analysis is the key subject for the structure engineering design. Therefore, to facilitate the use of AAF in reinforced concrete, more studies on mechanical properties, such as compressive strength and splitting tensile strength, need to be carried out.

This paper tries to analyze and compare the mechanical properties of common SFRC and AAFRC, such as slump, compressive strength, splitting tensile strength, flexural strength, tension-compression ratio, and toughness index. SEM analysis was carried out on AAFRC and SFRC to observe the bond performance of the matrix and fibers. Empirical equations used to predict the compressive strength and flexural strength of AAFRC were proposed and discussed.

2. Experimental Programs

2.1. Materials. In this study, ordinary Portland cement (OPC) was obtained from the Conch Cement Pvt. Ltd, China. Its properties are presented in Table 1, which were determined according to BS EN 197-1 [19]. Fly ash is of II grade level [20]. The characteristics of fly ash are given in Table 1. Natural river sand was used as the fine aggregate. The particle size distribution and physical properties of fine aggregates are presented in Table 2. The coarse aggregate used was calcareous crushed stone with 2.5 cm of the maximum size. Concrete mixture proportions used in the study are given in Table 3.

Table 4 shows the properties of the AAF and SF used in the study; both of them are 35 mm in length since the mold section of 100 × 100 mm was chosen for strength tests based on CECS 13-2009 [21]. The width of AAF is 2 mm. Figure 1 shows the appearance and flexibility of the AAF. It can be seen that the AAF shows an extremely thin strip shape with good toughness. The AAF and SF were mixed in volume fractions of 0%, 0.2%, 0.4%, 0.6%, 0.8%, and 1.0%, respectively.

2.2. Mixing and Curing. First, the coarse and fine aggregates were added and dry mixed for 1 min. Then, the dry mixing of the cement was conducted for another 1 min. Fibers were then added into the dry mixture and mixed for another 1 min. Finally, water was added slowly. To ensure an even dispersion of fibers in the concrete, the mixing of the fresh concrete was carried out for 3 min. The fresh concrete was cast into 100 × 100 × 400 mm prismatic molds for the flexural strength test and into 100 × 100 × 100 mm cube molds for the compressive strength test and splitting tensile strength test separately. After casting, the produced specimens were cured in air at 20 ± 2°C in molds covered by a polyethylene film to prevent moisture loss. After 24 h, the samples were removed from the molds and transferred to a standard condition with T = 20 ± 2°C and RH = 95 ± 5% until the testing age. In this study, every test result consisted of the average of three replicate tests.

2.3. Testing Methods

2.3.1. Slump. The test of slump was carried out according to the standard GB/T 50080-2002 [22]. The fresh concrete was

Table 1: Properties of OPC and fly ash.

Chemical composition (wt.%)	Cement (OPC)	Fly ash
CaO	61.25	2.34
SiO_2	20.58	54.82
Al_2O_3	5.64	32.2
Fe_2O_3	3.95	3.66
MgO	2.48	1.08
Na_2O	0.36	0.12
K_2O	—	0.37
SO_3	3.18	—
TiO_2	0.12	—
Loss on ignition	—	5.41
Physical properties		
Specific gravity (g/cm^3)	3.10	2.31
Specific surface area (m^2/kg)	385	3120
Fineness modulus	—	—
Initial setting time (min)	90	—
Final setting time (min)	185	—

Table 2: Particle size distributions and physical properties of sand.

Sieve size (mm)	Cumulative percentage retained (%)
5.0	5
2.50	14
1.25	21
0.63	41
0.315	85
0.160	98
Apparent density (kg/m^3)	2700
Bulk density (kg/m^3)	1450
Specific gravity (kg/m^3)	1600
Saturated surface water absorption (%)	0.80

Table 3: Concrete mixture proportions used in the study.

Cement (kg/m^3)	Fly ash (kg/m^3)	Fine aggregate (kg/m^3)	Coarse aggregate (kg/m^3)	Water (kg/m^3)
450	128	625	1025	270

Table 4: Properties of AAF and SF.

Fiber variety	AAF	SF
Modulus of elasticity (MPa)	14×10^4	20×10^4
Density (g/cm^3)	7.20	7.85
Length (mm)	35	35
Tensile strength (MPa)	2000	1100
Elongation (%)	—	3.5
Acid/alkali resistance	High	Low
Electrical conductivity	High	High
Component	Amorphous metal $(Fe,Cr)_{80}(P,C,Si)_{20}$	Alloy

filled into the slump tube and was flushed out from top of the tube. Afterwards, the slump tube was lifted in 5–10 s. The slump value was calculated by subtracting the height of the highest point of the slumped concrete from the height of the tube.

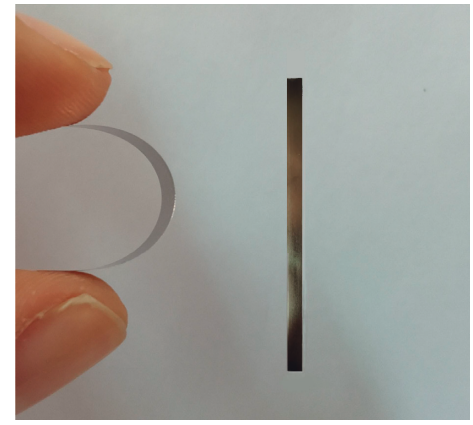

Figure 1: The appearance and flexibility of AAF.

2.3.2. Compressive Strength and Splitting Tensile Strength. The compressive strength and splitting tensile strength of cube specimens were tested according to GB/T 50081-2002 and SL 352-2006 [23, 24], at the curing periods of 7, 28, and 90 days, respectively.

2.3.3. Flexural Strength and Toughness Index. Flexural strength at 7, 28, and 90 days was, respectively, tested according to CECS 13-2009 through the four-point bending experiments conducted on the universal testing machine (Model SHT4305). The $100 \times 100 \times 400$ mm sized specimens were fabricated and tested. The span of the flexural experiment was 300 mm. The load was applied by a displacement control with a rate of 0.1 mm/min. The flexural strength was determined using the following equation:

$$f = \frac{F_{\max} l}{bh^2}, \quad (1)$$

where f is the flexural strength (MPa), $F_{\max}$ is the maximum load (N), l is the span length (mm), b is the width of the specimen cross section (mm), and h is the height of the specimen cross section (mm) [21].

2.3.4. SEM Analysis. SEM analysis was carried out on AAFRC and SFRC specimens cured for 28 days separately to observe the interfacial bond between the matrix and fibers. The microstructures of the samples were tested by JSM-5900 SEM manufactured by JEOL in Japan.

3. Results and Discussion

3.1. Slump. The FRC's slump measurements are shown in Table 5. The results show that the slump values of reinforced concrete decrease as the fiber volume fraction increases. For the plain concrete, the slump is 135 mm. When adding SFs with a volume fraction of 0.2%, 0.4%, 0.6%, 0.8%, and 1.0%, the slump of SFRC specimens decreases to 130 mm, 126 mm, 124 mm, 120 mm, and 118 mm, respectively, and the slump of AAFRC falls down to 123 mm, 110 mm, 100 mm, 95 mm, and 80 mm, respectively. This could be due to the amount of cement used to coat the coarse and fine aggregates being

Table 5: Results of slump and compressive strength tests.

Mixture no.	Fiber length (mm)	V_f (%)	Slump (mm)	Compressive strength (MPa)					
				7 d		28 d		90 d	
				Measured (MPa)	Strength-effectiveness (%)	Measured (MPa)	Strength-effectiveness (%)	Measured (MPa)	Strength-effectiveness (%)
C0	—	0	135	36.5 (±1.76)	—	42.3 (±2.21)	—	53.4 (±2.23)	—
SF1	35	0.2	130	38.7 (±1.86)	6.12	44.3 (±2.43)	4.81	55.2 (±2.92)	3.35
SF2		0.4	126	40.6 (±2.42)	11.31	45.5 (±2.69)	7.56	56.4 (±3.03)	5.65
SF3		0.6	124	41.6 (±3.03)	14.22	46.6 (±2.37)	10.23	58.1 (±2.53)	8.78
SF4		0.8	120	42.5 (±2.92)	16.47	47.9 (±2.78)	13.21	60.1 (±2.60)	12.56
SF5		1.0	118	46.2 (±3.00)	19.45	49.2 (±2.29)	16.45	61.1 (±2.77)	14.56
AF1	35	0.2	123	38.9 (±2.45)	6.52	45.7 (±1.84)	8.21	56.0 (±2.00)	4.87
AF2		0.4	110	41.0 (±2.87)	12.31	46.9 (±1.89)	11.01	57.5 (±2.38)	7.65
AF3		0.6	100	42.2 (±2.56)	15.62	48.3 (±2.09)	14.12	59.3 (±2.88)	9.12
AF4		0.8	95	42.4 (±2.24)	16.12	48.8 (±2.15)	15.41	60.2 (±2.54)	12.78
AF5		1.0	80	43.0 (±1.97)	17.87	49.4 (±2.45)	16.72	59.4 (±2.16)	11.21

Note: strength-effectiveness (%) = [(strength of fiber concrete − strength of pure concrete)/strength of pure concrete] × 100%.

relatively reduced due to the addition of fibers. A portion of the cement is required to cover the surface of fibers, affecting the slump values. The network structure of fibers increases the friction within the mixture and reduces its workability as well. Kim et al. [25] drew a similar conclusion, where the amount of slump decreased as the amorphous metallic fiber volume fraction was increased.

It can also be seen that the slump of AAFRC decreases more obviously than that of SFRC with the same volume fraction. The AAF has a greater specific surface area due to its thin plate shape, and the large numbers of such fibers are mixed into the concrete, thus leading to a lower flowability.

3.2. Compressive Strength. Table 5 shows the compressive strength and strength-effectiveness of the specimens at 7, 28, and 90 days, respectively. Generally, the addition of AAF contributes to an increase in the compressive strength of concrete. When adding AAF with the volume fraction of 0.2%, 0.4%, 0.6%, 0.8%, and 1.0%, the compressive strength of the specimens has an increase of 8.21%, 11.01%, 14.12%, 15.41%, and 16.72%, respectively, at 28 days. Correspondingly, the compressive strength improvement of the specimens reinforced with SF is 4.81%, 7.56%, 10.23%, 13.21%, and 16.45%, respectively.

As the volume fraction increases, the compressive strength of SFRC gains a continuous improvement. This could be due to the higher unit volume quantity of AAF than SF, which causes a larger contact area with the concrete matrix, helping the FRC to sustain larger compression force. Table 6 shows the comparison of fiber quantity per cubic meter and fiber specific surface area (FSS). It can be seen from the table that the number of AAFs per unit volume is 3.8 times the number of SFs and the FFS is 9.76 times. In the FRC with the same fiber content, AAF can maintain more effective bonding with the matrix than SF.

Meanwhile, when the compression is perpendicular to fibers, the microcrack can be delayed by the bridging process. However, when the fibers are parallel to the compression, debonding is likely to occur at the interface of the matrix and fibers. It will be difficult to counteract the damage [26]. This phenomenon is more significant: when the amount of AAF is excessive, the smooth surface and inhomogeneous dispersion of AAF intensify the formation of defects on the excessive contact area, which counteracts the enhancement effect; that is why the change of compressive strength-effectiveness of AAFRC is not obvious when the volume fraction exceeds 0.8%. Yoo et al. [27] found the similar results that the compressive strength of the specimens added with 0.5% AAF was 11.3% greater than that of the plain ones at 28 days. However, when fiber content increased from 0.5% to 0.75%, the compressive strength increased by only 1.23%. The strength-effectiveness decreased significantly when AAF content approached 0.8%. In contrast, they found that the compressive strength increased slightly with the increase of SF percentage and concluded that a lower number of SFs included in the mixture attributed to better dispersion compared to AAFs. Furthermore, the compressive strength is also related to the hydration of cement, fiber distribution, and the bond between fiber and aggregate, cement matrix. As it was indicated by previous researchers [26, 28, 29], the bond strength between matrix and fibers has not been evidently explored and thus does not provide evidence in regard to the development of the compressive strength of FRC.

3.3. Splitting Tensile Strength. Figure 2 shows the strength-effectiveness of the splitting tensile strength of the concrete specimens at 28 days. Compared with the plain concrete, the splitting tensile strength of FRC increases significantly with the added content of fibers. As the fiber content increased, the splitting tensile strength of AAFRC increases in a range from 10.4% to 32.8%, whereas the splitting tensile strength of SFRC increases in a range from 5.6% to 21.07%. A previous research on PP hybrid and basalt FRC also showed significant improvement on splitting tensile strength [30, 31]. Once the first crack occurs, the specimen is not destroyed instantaneously, as the fiber can bear the load transferred by the matrix cracking. Due to the interface bonding between the fiber itself and the matrix, the loading capacity continues to rise despite the stable crack propagation. FRC does not reach ultimate tensile strength before fast crack propagation.

Table 6: Comparison of the number of fibers per cubic meter.

Fiber variety	Surface area of single fiber (cm^2)	Volume of single fiber (cm^3)	Fiber quantity per cubic meter	FSS (cm^{-1})
AAF	0.649	0.000832	12,019,230	780.0
SF	0.251	0.00314	3,184,713	79.9

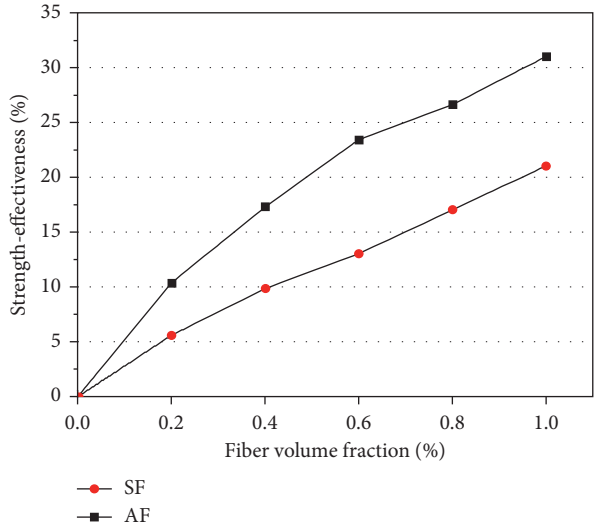

Figure 2: Splitting strength-effectiveness of FRC.

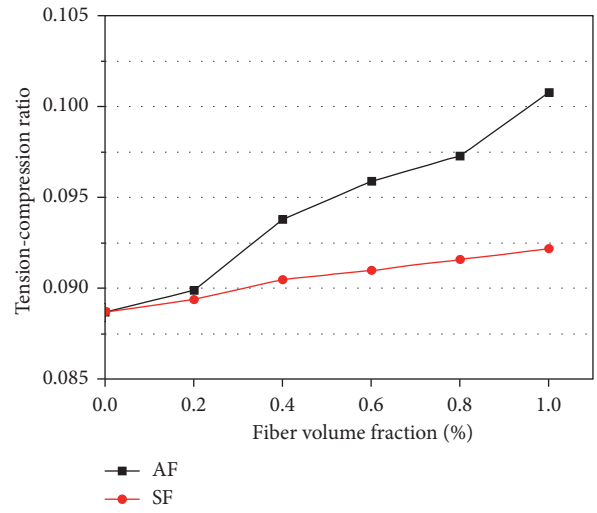

Figure 3: Tension-compression ratio of FRC.

The test results also notice that the AAFRC shows better splitting tensile strength than the SFRC. The thin plate shape is good for AAFs to include more amounts in the mixture than SFs with the same volume content. The splitting tensile strength of FRC is proportional to the number of fibers intersecting the fracture surfaces [32]. Furthermore, the tensile strength of AAF is 2000 MPa, while that of SF is 1100 MPa, which benefits the splitting tensile strength of AAFRC.

High-strength concrete has high brittleness, which causes it to crack when the temperature changes violently. Brittleness is an important index to measure concrete performance. The tension-compression ratio can represent the brittleness of concrete [33, 34]; the greater the ratio, the smaller the brittleness. Figure 3 shows the tension-compression ratio of the concrete specimens. The ratio grows steadily with the increase of the fiber amount. Adding both AAF and SF decreases the brittleness of concrete. It is worth noting that adding AAF is much better for suppressing the brittleness, and AAF can also effectively improve the ductility of concrete.

3.4. Flexural Strength. The result of the flexural strength test is given in Table 7, including the flexural strength and strength-effectiveness of FRC at 7, 28, and 90 days. Compared with the plain concrete, the increase of flexural strength of the specimens reinforced with SF ranges from 6.12% to 17.45% at 7 days, while that of the AAF specimens ranges from 20.32% to 47.21%. Compared with the plain concrete, the strength-effectiveness of SF specimens is 5.21%, 7.56%, 9.23%, 12.21%, and 14.15% with the volume fraction of 0.2%, 0.4%, 0.6%, 0.8%, and 1.0% at 28 days, and the corresponding ratio of AAF specimens is 18.12%, 27.54%, 36.78%, 40.21%, and 45.21%. The addition of both SFs and AAFs can improve the flexural strength of FRC. Previous studies reported that the flexural strength of FRC with the hooked steel, polypropylene, glass, and polyester fibers improved by 15.7%, 7.6%, 14.4%, and 21.3%, respectively, at a fiber content of 0.5 kg/m^2 [35]. Compared with the plain concrete, FRC has higher flexural strength.

Furthermore, the result of the tests shows that the flexural properties of AAFRC are superior to those of SFRC, compared with common fibers, such as hooked steel, PP, and glass fibers; AAF also showed an obvious advantage in improving the flexural strength of FRC. As a single fiber, the straight-shaped AAF is less resistant to adhesion with matrix under pull-out load compared with hooked-type SF [5], but at the same volume fraction, the larger number and higher tensile strength may help AAFs carry more stress from the matrix after flexural cracking.

3.5. Toughness Index. The load-deflection curves of the plain concrete, SFRC, and AAFRC samples with the volume fraction of 0.4% and 0.8%, respectively, are shown in Figure 4. The addition of fibers delays the first crack significantly, compared with the plain concrete, and concrete reinforced with fibers could also take a greater load before the initial cracking. On the contrary, the plain concrete showed its brittleness, as the load decreases rapidly with increasing deflection after peak load. However, the AAFRC behaved better, which can be seen from the flatter curves. The AAF with high tensile strength can act like bridges and

Table 7: Result of flexural strength tests.

Mixture no.	Fiber length (mm)	V_f (%)	Flexural strength (MPa)					
			7 d		28 d		90 d	
			Measured (MPa)	Strength-effectiveness (%)	Measured (MPa)	Strength-effectiveness (%)	Measured (MPa)	Strength-effectiveness (%)
C0	—	0	4.01 (±0.23)	—	4.63 (±0.16)	—	5.74 (±0.35)	—
SF1	35	0.2	4.25 (±0.19)	6.12	4.87 (±0.21)	5.21	5.97 (±0.43)	4.15
SF2		0.4	4.34 (±0.26)	8.31	4.98 (±0.37)	7.56	6.12 (±0.58)	6.65
SF3		0.6	4.42 (±0.26)	10.22	5.05 (±0.32)	9.23	6.21 (±0.45)	8.18
SF4		0.8	4.59 (±0.32)	14.47	5.19 (±0.34)	12.21	6.30 (±0.51)	9.86
SF5		1.0	4.71 (±0.27)	17.45	5.28 (±0.45)	14.15	6.40 (±0.69)	11.56
AF1	35	0.2	4.82 (±0.34)	20.32	5.47 (±0.35)	18.12	6.65 (±0.50)	15.87
AF2		0.4	5.21 (±0.31)	29.85	5.91 (±0.48)	27.54	7.15 (±0.70)	24.65
AF3		0.6	5.54 (±0.43)	38.14	6.33 (±0.52)	36.78	7.47 (±0.77)	30.12
AF4		0.8	5.74 (±0.39)	43.21	6.49 (±0.53)	40.21	7.79 (±0.63)	35.78
AF5		1.0	5.90 (±0.50)	47.21	6.72 (±0.65)	45.21	7.93 (±0.75)	38.21

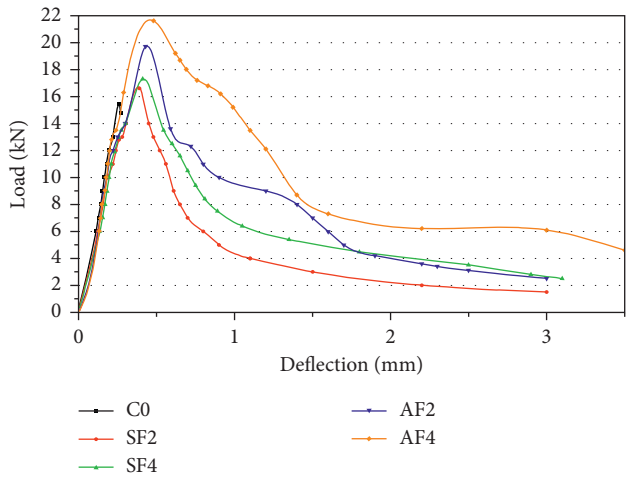

Figure 4: The load-deflection curves of FRC.

absorb destructive energy from the matrix, which restrains the concrete from completely fracturing after the first crack. As a comparison, for the SFRC, the improvement of brittle fracture resistance was not significant.

The toughness index is denoted by the ratio of area under the load-deflection curve up to the specific deflections (δ, 3δ, 5.5δ, and 10.5δ) to the area up to the deflection (δ) at the first flexural cracking, as shown in figure of Table 8 [24]. The toughness indexes are termed as I_5 at 3δ, I_{10} at 5.5δ, and I_{30} at 15.5δ. It can be seen from Table 7 that the toughness indexes of FRC increased compared with the plain concrete, and the FRC with AAF showed the finest toughness improvement capacity. For example, toughness indexes I_5, I_{10}, and I_{30} of SF4-reinforced concrete are 3.68, 4.88, and 6.14, respectively. These three toughness indexes of AF4-reinforced concrete are 4.70, 6.97, and 9.93, showing apparent increases compared with the values of the plain concrete. On the contrary, it was also observed that the cracks are more closely spaced in all the fiber concrete beams and that the crack width was consequently less in these beams compared to that in the plain beams.

3.6. Prediction of Flexural Strength and Compressive Strength. Predicting the flexural strength and compressive strength of FRC is an important study in terms of limits on the deflection and crack width control. An empirical equation based on compressive strength of the plain concrete and fiber-reinforcing index is suggested to predict the strength of steel fiber-reinforced concrete [36]:

$$f_{\mathrm{SFRC}} = A\left(f'_{\mathrm{cu}}\right)^{\alpha_1} + B\left(f'_{\mathrm{cu}}\right)^{\alpha_2}\mathrm{RI} + C\mathrm{RI}, \quad (2)$$

where f_{SFRC} is the strength property of the SFRC; f'_{cu} is the 28-day compressive strength of the plain concrete; A, B, and C are regression coefficients; and RI is the fiber-reinforcing index ($V_f L_f/\varphi_f$), in which V_f is the volume fraction of the fiber and L_f/φ_f is the fiber aspect ratio. The first term with coefficient A represents the contribution of strength of the plain concrete of matrix. The second term with coefficient B represents the contribution of matrix strength-fiber interaction explicitly. The third term with coefficient C represents the contribution of the fiber dosage and fiber geometry.

With reference to this equation, the values of α_1 and α_2 and coefficient C can be referred from the strength prediction models of SFRC, the coefficients of A and B can be determined by fitting the results of the flexural strength test, as shown in Figure 5. The empirical equation is suggested to predict the flexural strength of AAFRC:

$$f_{\mathrm{flF}} = 0.810\left(f'_{\mathrm{cu}}\right)^{0.5} - 0.147\left(f'_{\mathrm{cu}}\right)^{0.5}\mathrm{RI} + 1.117\mathrm{RI}. \quad (3)$$

Correlation coefficient $R2$ of 0.95 shows significant correlation.

Figure 6 shows the comparison of predicted and experimental values of compressive strength. The empirical prediction equation of compressive strength can be obtained as follows:

$$f_{\mathrm{cuF}} = 1.065 f'_{\mathrm{cu}} - 0.014 f'_{\mathrm{cu}}\mathrm{RI} + 1.09\mathrm{RI}. \quad (4)$$

The correlation coefficient $R2$ is 0.94.

3.7. SEM Analysis. To observe the microstructure bonding characteristic of SFRC and AAFRC at 28 days, the SEM patterns of SFRC and AAFRC are shown in Figure 7. It

Table 8: Toughness index of FRC.

Mixture no.	I_5	I_{10}	I_{30}
C0	1.00	1.00	1.00
SF1	2.51	3.24	4.13
SF2	2.75	3.61	4.65
SF3	3.12	4.08	5.10
SF4	3.68	4.88	6.14
SF5	4.35	5.61	6.78
AF1	3.54	5.12	6.01
AF2	4.04	6.02	7.65
AF3	4.31	6.54	8.35
AF4	4.70	6.97	9.93
AF5	5.20	7.10	10.20

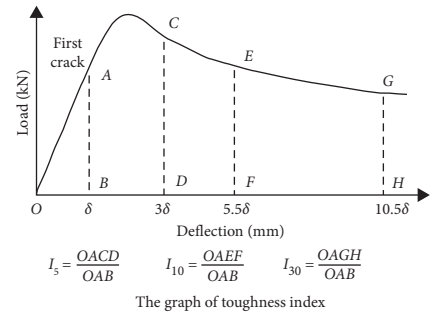

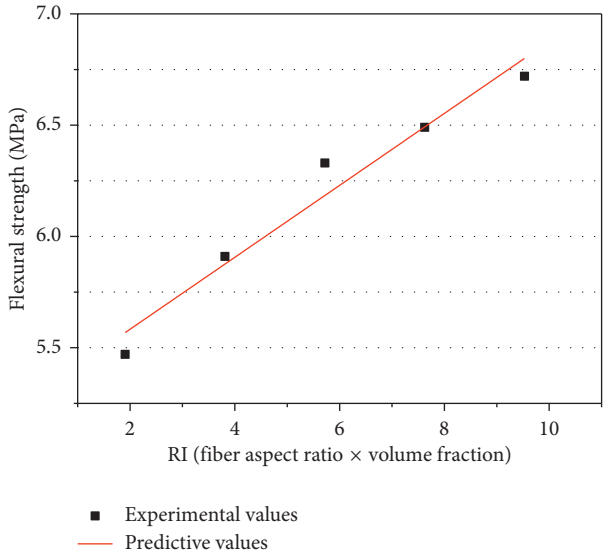

Figure 5: Comparison of predicted and experimental values of flexural strength.

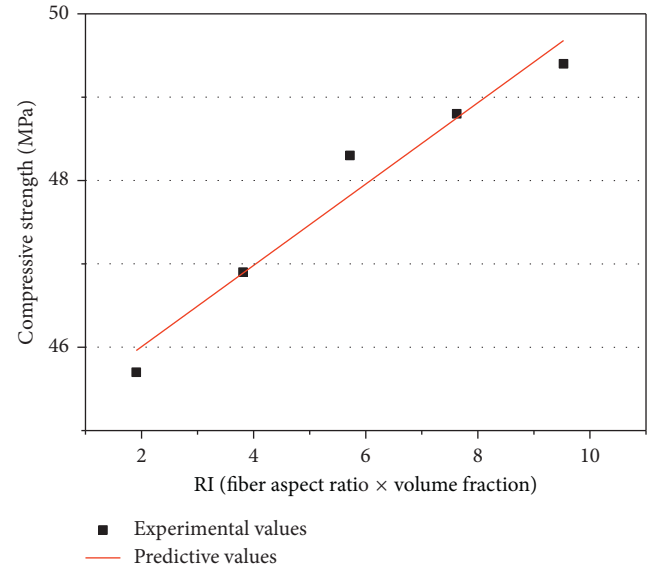

Figure 6: Comparison of predicted and experimental values of compressive strength.

can be seen from the patterns that the SF has bonded to the matrix and attached to a large amount of hydration products; this phenomenon implies a substantial interfacial bond between SF and cement matrix. Meanwhile, it can be seen from Figure 7(b) that the AAF is covered with a great number of hydration products. Density and low porosity are obtained in the fiber-matrix interface, favoring the contact of the C-S-H gel with AAF. The addition of AAF can prevent the initiation and propagation of cracks effectively and improve the mechanical properties of cement-based materials which implies that AAF and cement show a good bonding performance.

4. Conclusions

This study worked on the mechanical properties of AAFRC and chose SFRC for comparison. The following conclusions are drawn by comparing and analyzing the testing results:

(1) The results obtained show that adding AAF can slightly decrease the slump of concrete. The addition of AAF improves the mechanical properties of concrete significantly, compared with the plain concrete, and the compressive strength and splitting tensile strength of AAFRC increase by 8.21–16.72% and 10.4–32.8%, respectively, while the compressive strength and splitting tensile strength of SFRC increase by 4.81–16.45% and 5.6–21.07%, respectively, with the same volume fraction. Compared to the SF, adding AAF can effectively improve the brittle characteristics of concrete.

(2) AAF shows an obvious advantage in improving the flexural strength of FRC compared with other fibers. The high tensile strength may help AAFs carry more stress from the matrix after flexural cracking. Meanwhile, the addition of fiber significantly improves the toughness index of concrete, as the AAFRC shows a greater resilience improvement. The AAF with

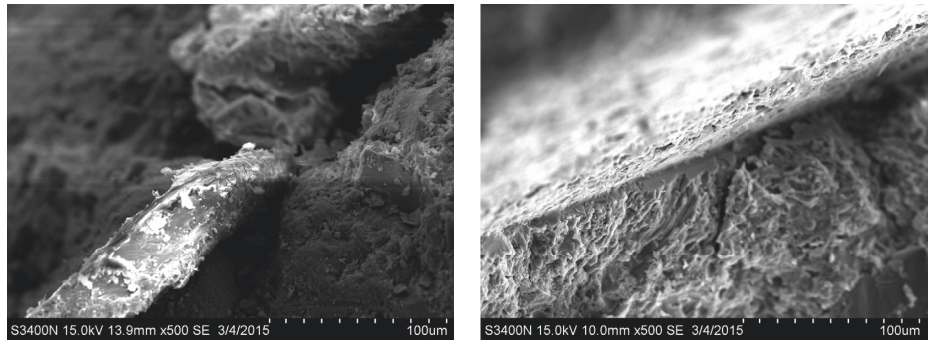

(a) (b)

Figure 7: SEM patterns of SFRC (a) and AAFRC (b) at 28 days.

high tensile strength acts like a bridge and absorbs destructive energy from the matrix, which restrains the concrete from completely fracturing after the first crack.

(3) SEM images of the microstructure show that a significant bond between the AAF surface and the hydrated cement matrix is obtained. Equations were suggested for predicting the flexural strength and compressive strength of AAFRC. The predictive and experimental values were compared, and the correlations were both significant, with coefficients of 0.95 and 0.94, respectively.

Generally, the addition of AAF benefits the mechanical properties of concrete. The concrete reinforced with AAF can afford greater strength restraint from cracking. Meanwhile, compared with other common FRC, AAFRC shows an advantage in many ways. This new-type fiber could be suitable for the preparation of high-performance concrete and application in many fields especially in marine environments such as port engineering. Therefore, AAFRC should be considered as a material with great prospects. For further research, the fibers with similar size and mechanical properties can be compared to reveal more enhancement mechanism of AAF on FRC.

Data Availability

The data used to support the findings of this study are included within the article.

Conflicts of Interest

The authors declare that they have no conflicts of interest.

Acknowledgments

This work described in this paper was supported by the Natural Science Foundation of Jiangsu Province (no. BK20151496) and the Postgraduate Research & Practice Innovation Program of Jiangsu Province (no. KYCX18_0608).

References

[1] H. Gholizadeh and S. Dilmaghani, "The study of mechanical properties of high strength concrete containing steel and polypropylene fibers," *Civil Engineering Journal*, vol. 4, no. 1, p. 221, 2018.

[2] C. Frazão, J. Barros, A. Camões et al., "Corrosion effects on pullout behavior of hooked steel fibers in self-compacting concrete," *Cement and Concrete Research*, vol. 79, pp. 112–122, 2016.

[3] J. Zhang, H. T. Zhong, X. C. Ju et al., "Comparative study on Cl^- penetration in cracked high ductility and low shrinkage material and steel fiber concrete," *Journal of Building Materials*, vol. 15, no. 2, pp. 151–157, 2012.

[4] I. Y. Pyshmintsev, A. N. Boryakova, and M. A. Smirnov, "Effect of cooling rate on the structure and properties of low-carbon tube steel," *Metallurgist*, vol. 52, no. 7-8, pp. 464–469, 2008.

[5] J. P. Won, B. T. Hong, S. J. Lee et al., "Bonding properties of amorphous micro-steel fibre-reinforced cementitious composites," *Composite Structures*, vol. 102, pp. 101–109, 2013.

[6] J. M. Yang, J. K. Kim, and D. Y. Yoo, "Effects of amorphous metallic fibers on the properties of asphalt concrete," *Construction and Building Materials*, vol. 128, pp. 176–184, 2016.

[7] P. Yu, B. A. Sun, H. Y. Bai et al., "Exploring plastic metallic glasses," *Physics*, vol. 37, no. 6, pp. 421–425, 2008.

[8] K. Friedrich, A. Fels, and E. Hornbogen, "Fatigue and fracture of metallic glass ribbon/epoxy matrix composites," *Composites Science and Technology*, vol. 23, no. 2, pp. 79–96, 1985.

[9] R. U. Vaidya and K. N. Subramanian, "Metallic glass ribbon-reinforced glass-ceramic matrix composites," *Journal of Material Science*, vol. 25, no. 7, pp. 3291–3296, 1990.

[10] Z. W. Wu, Z. C. Lu, X. J. Ni et al., "Effect of heat treatment on corrosion behaviour of amorphous metal fibers," *Journal of Iron and Steel Research*, vol. 21, no. 11, pp. 1030–1034, 2014.

[11] S. J. Choi, B. T. Hong, S. J. Lee et al., "Shrinkage and corrosion resistance of amorphous metallic-fiber-reinforced cement composites," *Composite Structures*, vol. 107, pp. 537–543, 2014.

[12] J. P. Won, B. T. Hong, T. J. Choi et al., "Flexural behaviour of amorphous micro-steel fibre-reinforced cement composites," *Composite Structures*, vol. 94, no. 4, pp. 1443–1449, 2012.

[13] B. J. Kim, C. K. Yi, and Y. R. Ahn, "Effect of embedment length on pullout behavior of amorphous steel fiber in Portland cement composites," *Construction and Building Materials*, vol. 143, pp. 83–91, 2017.

[14] S. C. Peng, M. L. Chen, and Q. C. Hou, *Preparation of Modified Amorphous Alloy Fiber Reinforced Concrete Composite Material*, CN200710052162.X, China, 2007.

[15] M. Naka and I. Okamoto, "Amorphous alloy and its application to joining," *Transactions of Jwri*, vol. 14, pp. 385–395, 2013.

[16] X. Wang, X. Chen, T. Xia et al., "The current situation of amorphous alloy application," *Materials Review*, vol. 20, no. 10, pp. 75–79, 2006.

[17] Z. C. Lu, Z. W. Wu, X. J. Ni et al., *Amorphous Alloy Fiber used for Concrete and Preparation Method of Amorphous Alloy Fiber*, CN201310435060.X, China, 2013.

[18] J. M. Yang, H. O. Shin, and D. Y. Yoo, "Benefits of using amorphous metallic fibers in concrete pavement for long-term performance," *Archive of Cibil and Mechanical Engineering*, vol. 17, no. 4, pp. 750–760, 2017.

[19] *BS EN 197-1 Cement, Composition, Specifications and Conformity Criteria for Common Cements*, European Committee for Standardization, London, UK, 2011.

[20] *GB/T. 50146-2014 Technical Code for Application of Fly Ash Concrete*, Ministry of Housing and Urban-Rural of the PRC, China Architecture & Building Press, China, 2014.

[21] *CECS 13-2009 Standard Test Method for Fiber Reinforced Concrete*, China Plan Press, China, 2010.

[22] *GB/T. 50080-2002 Standard for Test Method of Performance on Ordinary Fresh Concrete*, Ministry of Construction of the PRC, China Architecture and Building Press, Beijing, China, 2003.

[23] *GB/T 50081-2002 Standard for Test Method of Mechanical Properties on Ordinary Concrete*, Ministry of Construction of the PRC, China Architecture and Building Press, Beijing, China, 2003.

[24] *SL 352-2006 Test Specifications of Hydraulic Concrete*, China Water Power Press, Beijing, China, 2006.

[25] H. Kim, G. Kim, J. Nam et al., "Static mechanical properties and impact resistance of amorphous metallic fiber-reinforced concrete," *Composite Structures*, vol. 134, pp. 831–844, 2015.

[26] C. Redon and J. L. Chermant, "Damage mechanics applied to concrete reinforced with amorphous cast iron fibers, concrete subjected to compression," *Cement and Concrete Composites*, vol. 21, no. 3, pp. 197–204, 1999.

[27] D. Y. Yoo, B. Bantnia, J. M. Yang et al., "Size effect in normal- and high-strength amorphous metallic and steel fiber reinforced concrete beams," *Construction and Building Materials*, vol. 121, pp. 676–685, 2016.

[28] J. C. Lee, W. J. Kim, and C. J. Lee, "Compressive properties of amorphous metal fiber reinforced concrete exposed to high temperature," *Journal of Korea Institute of Building Construction*, vol. 12, no. 2, 2012.

[29] G. T. Truong, K. K. Choi, and O. C. Choi, "Tensile and compressive creep behaviors of amorphous steel fiber-reinforced concrete," *Journal of Recycled Construction Resources*, vol. 1, no. 3, pp. 197–203, 2013.

[30] M. Hsie, C. Tu, and P. S. Song, "Mechanical properties of polypropylene hybrid fiber-reinforced concrete," *Materials Science and Engineering A*, vol. 494, no. 1-2, pp. 153–157, 2008.

[31] C. H. Jiang, K. Fan, F. Wu et al., "Experimental study on the mechanical properties and microstructure of chopped basalt fibre reinforced concrete," *Materials and Design*, vol. 58, no. 6, pp. 187–193, 2014.

[32] J. Potrzebowski, "The splitting test applied to steel fibre reinforced concrete," *International Journal of Cement Composites and Lightweight Concrete*, vol. 5, no. 1, pp. 49–53, 1983.

[33] W. Li, Z. Huang, X. C. Wang et al., "Study on tension and compression ratio and discount ratio of rubber modified silica fume concrete," *Applied Mechanics and Materials*, vol. 670-671, pp. 396–400, 2014.

[34] R. Li, X. H. Zhang, and Y. F. Meng, "Study of performance on reduce fragility and increase the toughness of fly ash ceramsite concrete," *Advanced Materials Research*, vol. 997, pp. 120–123, 2014.

[35] A. Sivakumar and M. Santhanam, "Mechanical properties of high strength concrete reinforced with metallic and non-metallic fibres," *Cement and Concrete Composites*, vol. 29, no. 8, pp. 603–608, 2007.

[36] J. Thomas and A. Ramaswamy, "Mechanical properties of steel fiber-reinforced concrete," *Journal of Materials in Civil Engineering*, vol. 19, no. 5, pp. 385–392, 2007.